Available online at www.sciencedirect.com
SCIENCE DIRECT®
Nuclear Physics B (Proc. Suppl.) 143 (2005) 205–210
NUCLEAR PHYSICS B PROCEEDINGS SUPPLEMENTS
www.elsevierphysics.com

Neutrino Magnetic Moments: Status and Prospects

Henry T. Wong[a]

[a]Institute of Physics, Academia Sinica, Taipei 11529, Taiwan.

Finite neutrino magnetic moments are consequences of non-zero neutrino masses. The particle physics foundations of the subject are summarized. The astrophysical bounds as well as the results from recent direct experiments are reviewed. Future projects and prospects are surveyed.

1. INTRODUCTION

The strong evidence of neutrino oscillations from the solar, atmospheric and long baseline accelerator and reactor neutrino measurements implies finite neutrino masses and mixings[1,2]. Their physical origin and experimental consequences are not fully understood. Experimental studies on the neutrino properties and interactions can shed light to these fundamental questions and provide constraints to the interpretations in the future precision oscillation experiments. New and improved neutrino sources and detector technologies have to be developed in parallel for such studies.

The couplings of neutrinos with the photons are generic consequences of finite neutrino masses, and are one of the important intrinsic neutrino properties[3] to explore. The neutrino electromagnetic vertex can be parametrized by terms with γ_η and $\sigma_{\eta\xi}$ corresponding to interactions without and with its spin, respectively identified as the "neutrino charge radius" and "neutrino magnetic moments", the latter of which is the subject of this review.

2. PARTICLE PHYSICS OVERVIEW

The effective Lagrangian for the spin component of the neutrino electromagnetic vertex can be described by

$$L = \frac{1}{2}\bar{\nu}_j \sigma_{\eta\xi}(\beta_{ij} + \epsilon_{ij}\gamma_5)\nu_i F^{\eta\xi} + h.c. \qquad (1)$$

where ϵ_{ij} and β_{ij} are respectively the electric and magnetic dipole moments which couple together the neutrino mass eigenstates $(\nu_i)_L$ and $(\nu_j)_R$, resulting in a change of the spin-state. Cases where $\nu_i{=}\nu_j$ and $\nu_i{\neq}\nu_j$ correspond to *diagonal* and *transitional* moments, respectively. Symmetry principles as well as neutrino properties place constraints to the matrices ϵ_{ij} and β_{ij}[4]. For example, Majorana neutrinos require $\epsilon_{ii}{=}\beta_{ii}{=}0$ which implies the diagonal moments vanishes. The study of neutrino electromagnetic properties is, therefore, in principle a way to distinguish between Dirac and Majorana neutrinos.

The experimental observable "neutrino magnetic moment" (μ_ν), usually expressed in units of the Bohr magneton $(\mu_{\rm B})$, for neutrinos with energy E_ν produced as ν_l at the source and after traversing a distance L can be described by

$$\mu_\nu^2(\nu_l, L, E_\nu) = \sum_j |\sum_i U_{li}\ e^{-iE_\nu L}\ \mu_{ij}|^2 \quad , \qquad (2)$$

where $\mu_{ij}{\equiv}|\beta_{ij} - \epsilon_{ij}|$ and U_{li} is the neutrino mixing matrix. The observable μ_ν is therefore an effective and convoluted parameter and the interpretations of experimental results depend on the exact ν_l compositions at the detectors. Accordingly, the μ_ν limits from reactor experiments, ^{8}B and ^{7}Be solar neutrino experiments are all different.

Given a specific model, μ_ν can be calculated from first principles. Minimally-Extended Standard Model with massive Dirac neutrinos[1] gives $\mu_\nu \sim 10^{-19}[m_\nu/1{\rm eV}]\mu_{\rm B}$ which is far too small to have any observable consequences. Incorporation of additional physics, such as Majorana neutrino transition moments or right-handed weak currents, can significantly enhance μ_ν to the experimentally relevant ranges[1,5]. Supersymmetry as well as extra-dimensions[6] can also contribute to the process.

0920-5632/$ – see front matter
doi:10.1016/j.nuclphysbps.2005.01.106

Information on μ_ν can be derived from astrophysics arguments as well as from direct laboratory experiments. A finite neutrino magnetic moment can be manifested in many processes[7]. In particular, studies of neutrino-electron scatterings are the most sensitive, robust and established methods. A finite μ_ν gives rise to an additional contribution in the ν-e scattering differential cross-section[5]

$$(\frac{d\sigma}{dT})_{\mu_\nu} \;=\; \frac{\pi\alpha_{em}^2}{m_e^2}[\frac{1-T/E_\nu}{T}]\;\mu_\nu^2 \qquad (3)$$

where T is the electron recoil energy, the experimental measurable. The neutrino radiative decay rate Γ_{ij} for the process $\nu_i \to \nu_j + \gamma$ is related to μ_{ij} and neutrino masses $m_{i,j}$ via[8]

$$\Gamma_{ij} = \frac{1}{8\pi}\frac{(m_i^2 - m_j^2)^3}{m_i^3}\mu_{ij}^2 \quad . \qquad (4)$$

3. ASTROPHYSICS BOUNDS

Astrophysics bounds on μ_ν were mostly derived from the consequences from a change of the neutrino spin-states in the astrophysical medium[1, 7]. These include studies in the available degrees of freedom in Big Bang Nucleosynthesis, stellar cooling via plasmon decay, and the cooling of supernova 1987a. The typical range is $\mu_\nu(astro) < 10^{-10} - 10^{-12}\mu_{\rm B}$.

The bounds, however, depend on modeling of the astrophysical systems, and on placing certain assumptions on the neutrino properties. The supernovae cooling arguments only apply for Dirac neutrinos where the right-handed state is sterile and can leave the astrophysical objects readily. Another generic assumption is the absence of other non-standard neutrino interactions except for the anomalous magnetic moments. For more realistic studies, a global treatment would be desirable, incorporating oscillation effects, matter effects as well as the complications due to interference and competitions among various channels.

The spin-flavor precession (SFP) mechanism, with or without matter resonance effects in the solar medium, has been used to explain solar neutrino deficit[9]. The solar ν_e would interact with solar magnetic field $\rm B_\odot$ via its magnetic moment to become $\nu_x (x \neq e)$. This scenario is in fact compatible with all solar neutrino data. The terrestrial KamLAND experiment, however, recently confirmed the Large Mixing Angle (LMA) parameter space of the matter oscillation scenario as *the* solution for the solar neutrino problem[1,2], such that SFP can be excluded as the dominant contribution in solar neutrino physics. Conversely, coupling the LMA allowed region with the recent KamLAND solar-$\bar{\nu_e}$ bounds of $\bar{\nu_e}/\nu_\odot < 2.8 \times 10^{-4}$[10], a constraint on $\int \mu_\nu[{\rm B}_{\odot\perp}]$ dr can be derived. Recent work on the modeling of $\rm B_\odot$[11] turned this into bounds on the magnetic moments, also in the range of $\mu_\nu(^8{\rm B}\text{-}\nu_\odot) < 10^{-10} - 10^{-12}\mu_{\rm B}$.

4. RECENT RESULTS FROM DIRECT EXPERIMENTS

Direct laboratory experiments on neutrino magnetic moments utilize solar, accelerator and reactor neutrinos as sources, and are conducted under controlled conditions. These approaches are robust and avoid the ambiguities and model-dependence in the astrophysical bounds. The experiments require an understanding of the neutrino energy spectra and compositions at the detectors by independent means. They typically study neutrino-electron scatterings $\nu_l + e \to \nu_x + e$. The signature is an excess of events over those due to Standard Model (SM) and other background processes, which exhibit the characteristic 1/T spectral dependence. Limits from negative searches are valid for both Dirac and Majorana neutrinos and for both diagonal and transitional moments. However, interpretations and comparisons among various experiments should take into account the difference in the flavor compositions between them *at* the detectors.

4.1. Solar Neutrinos

Data from the solar neutrino and KamLAND experiments firmly established the validity of the Standard Solar Model (SSM) predictions of the solar neutrino flux, as well as the LMA-matter oscillation solution being the leading mechanism of neutrino flavor conversion in the Sun. This can be used as the basis of magnetic moment searches

with solar neutrino data.

The Super-Kamiokande (SK) Collaboration performed spectral distortion analysis of their electron recoil spectral due to ^{8}B solar neutrino-electron scattering[12]. The study was to look for 1/T excess over an oscillation "background" at the 5-14 MeV energy range. SK data alone allowed a large region of $(\Delta m^2, tan^2\theta)$ parameter space and could only set limit of $\mu_\nu(^8\text{B-}\nu_\odot) < 3.6 \times 10^{-10}\mu_\text{B}$ at 90% Confidence Level (CL). Coupling with constraints from the other solar neutrino and KamLAND results, the LMA region is uniquely selected as *the* solution, such that a more stringent limit of $\mu_\nu(^8\text{B-}\nu_{\odot;LMA}) < 1.1 \times 10^{-10}\mu_\text{B}$ at 90% CL was derived.

The Borexino Collaboration performed analysis of their Counting Test Facility data at the ^{7}Be solar neutrino relevant range: 200−500 keV[13]. Subtracting the known ^{14}C β-spectrum and *assuming* an additional linear background, a fit to look for an 1/T spectrum did not indicate any excess and a limit of $\mu_\nu(^7\text{Be-}\nu_\odot) < 5.5 \times 10^{-10}\mu_\text{B}$ at 90% CL was derived, using SSM ^{7}Be $\nu_\odot$ flux.

An innovative insight is that neutrino magnetic moments can induce photo-dissociation in deuterium. The agreement between SNO neutral-current measurements with SSM $\nu_\odot$-flux predictions placed constraints of $\mu_\nu(^8\text{B-}\nu_\odot) < 3.7 \times 10^{-9}\mu_\text{B}$ at 95% CL[14].

4.2. Accelerator Neutrinos

Accelerators provide neutrinos with known flavor compositions. The timing structures can be used for background subtraction. Compared to reactor neutrinos, the lower flux as well as higher energy limit the sensitivities. However, neutrinos of all three flavors are produced at accelerators such that this is the only laboratory avenue for studying magnetic moments from ν_μ and ν_τ.

The LSND experiment measured "single electron" events from a beam with known ν_e, ν_μ and $\bar{\nu_\mu}$ fluxes and spectral compositions[15]. Taking the SM calculated values of $\sigma(\nu_\mu\text{-}e)$ and $\sigma(\bar{\nu_\mu}\text{-}e)$ which were confirmed by other experiments, the derived value of $\sigma(\nu_e\text{-}e)$ agreed well with SM predictions and provided a measurement of $sin^2\theta_W$=0.248 ± 0.051. Limits of $\mu_\nu(\nu_e) < 1.1 \times 10^{-9}$ μ_B and $\mu_\nu(\nu_\mu) < 6.8 \times 10^{-10}$ μ_B at 90% CL were derived from the absence of excess of counts.

The DONUT experiment first observed explicit ν_τ charged-current interactions[1] showing the ν_τ flux at a beam dump configuration is consistent with the expected level. The experiment also looked for "single-electron" events at cross-sections much larger than SM expectations. One event was observed while the predicted background from other known sources was 2.3[16]. This was converted into a magnetic moment limit for ν_τ: $\mu_\nu(\nu_\tau) < 3.9 \times 10^{-7}$ μ_B at 90% CL.

4.3. Reactor Neutrinos

Reactor neutrino experiments provide the most sensitive laboratory searches for the magnetic moments of $\bar{\nu_e}$, taking advantages of the high $\bar{\nu_e}$ flux, low E_ν and better experimental control via the reactor ON/OFF comparison. Neutrino-electron scatterings were first observed in the pioneering experiment[17] at Savannah River. A revised analysis of the data by Ref [5] with improved input parameters gave a positive signature consistent with the interpretation of a finite μ_ν at $\mu_\nu(\bar{\nu_e}) \sim 2 - 4 \times 10^{-10}$ μ_B.

The MUNU experiment[18] at the Bugey reactor in France deployed a Time Projection Chamber filled with 11.4 kg of CF_4 gas at 3 bar, surrounded by active liquid scintillator as anti-Compton vetos. It gave excellent single-electron event selection and measured the scattering angle with respect to the reactor core direction. Neutrino events are scattered "forward" such that a forward/backward comparison was used to subtract background. The residual spectra from 66.6 days of reactor ON data are shown in Figure 1. The residuals above T=900 keV were consistent with SM expectations, while an excess of events at 300 keV<T<900 keV was observed where the origins remain unknown. Various limits were evaluated depending on the threshold: $\mu_\nu(\bar{\nu_e}) < 1.7/1.4/1.0 \times 10^{-10}$ μ_B at 90% CL at 300, 700, 900 keV threshold, respectively. The low energy (<2 MeV) reactor neutrino spectra are not well-modeled[19] such that the possibility of yet-unaccounted-for neutrino production channels at the MeV range should be examined.

The TEXONO Collaboration adopted a compact all-solid design with a high-purity germa-

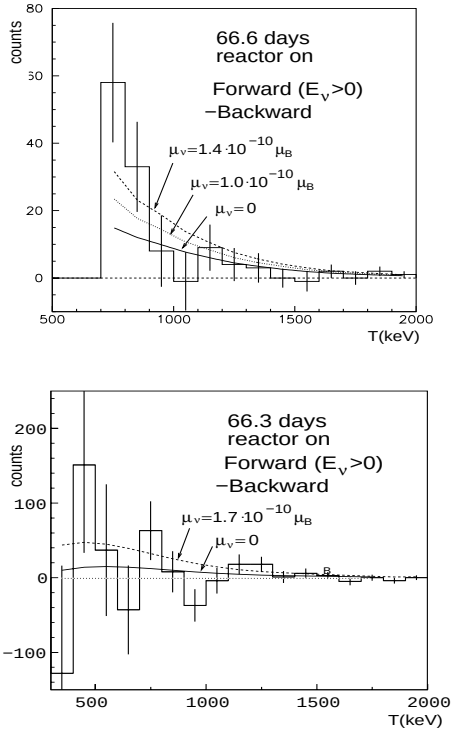

Figure 1. Reactor-ON forward minus background residual spectra from MUNU with visual (>700 keV) and automatic (>300 keV) scans.

nium detector(HPGe) 1.06 kg in mass, surrounded by anti-Compton detectors of NaI(Tl) and CsI(Tl) scintillators, radon shields, passive shielding materials, and plastic scintillators veto panels. The measurement was performed at the Kuo-Sheng(KS) Power Plant in Taiwan.

The focus was on the T=10-100 keV range for the enhanced signal rates and robustness in the control of systematic uncertainties. At this energy range, the ν-e scattering rates due to magnetic moments are much larger than the SM rates at the 10^{-10} $\mu_{\rm B}$ sensitivity level being explored, so that uncertainties in the irreducible SM background can be neglected[19]. In addition, $T \ll E_\nu$ such that the μ_ν-related scattering rates depend on the *total* neutrino flux (ϕ_ν) rather than the poorly-known details of the low-energy reactor neutrino spectra. The total neutrino flux is well-known and can be evaluated accurately from reactor operation data – every fission is expected to produce about 6 and 1.2 $\bar{\nu_e}$'s due to β-decays of the fission daughters and of ^{239}U following neutron capture on ^{238}U, respectively.

Comparing 4712/1250 hours of reactor ON/OFF data, no excess of events was found and with an analysis threshold of 12 keV just above the complications due to atomic effects, a limit of $\mu_\nu(\bar{\nu_e}) < 1.3 \times 10^{-10}$ $\mu_{\rm B}$ at 90% CL was derived. The ON/OFF and residual spectra are displayed in Figure 2. In addition, a background level of $\sim 1\ kg^{-1}keV^{-1}day^{-1}$ at the 10-20 keV range was achieved – a comparable range to those from the underground Dark Matter experiments.

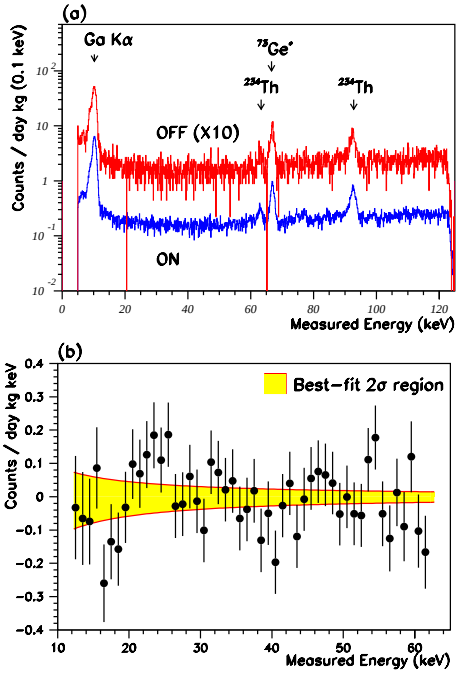

Figure 2. Energy spectra from TEXONO/KS: (a) reactor ON/OFF and (b) residual.

Depicted in Figure 3a is the summary of the results in $\mu_\nu(\bar{\nu_{\rm e}})$ searches versus the achieved threshold in reactor experiments. The dotted lines denote the R = $\sigma(\mu)/\sigma$(SM) ratio at a particular [T, $\mu_\nu(\bar{\nu_{\rm e}})$]. The large R-values for the KS experiment imply that its results are robust against the uncertainties in the SM cross-sections. In particular, if the excess events in Refs. [17] and [18] are due to unaccounted sources of neutrinos, the limits remain valid. Indirect bounds on the neutrino radiative decay lifetimes are inferred and displayed in Figure 3b for the scenario where a

single channel dominates the transition. It corresponds to $\tau_\nu m_\nu^3 > 9.5 \times 10^{18}$ eV^{3}s at 90% CL in the non-degenerate case. It can be seen that ν-e scatterings give much more stringent bounds than the direct searches[20].

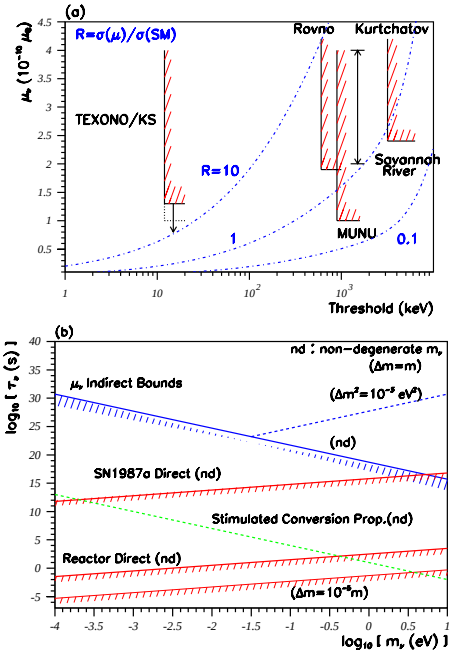

Figure 3. Summary of the results in (a) the searches of neutrino magnetic moments with reactor neutrinos, and (b) the bounds of neutrino radiative decay lifetime.

4.4. Global Analysis

A global analysis was performed[21] fitting simultaneously the magnetic moment data from the reactor and solar neutrino experiments, and the LMA oscillation parameters constrained by solar neutrino and KamLAND results. Only Majorana neutrinos were considered such that there were only transition moments. A "total" magnetic moment vector Λ=$(\mu_{23}, \mu_{31}, \mu_{12})$ was defined, such that its amplitude was given by $|\Lambda|^2$=$\frac{1}{2}Tr(\mu^+\mu)$. A global fit produced 90% CL limits of $|\Lambda| < 4.0\times10^{-10}\ \mu_B$ from solar and KamLAND data, and $|\Lambda| < 1.8\times10^{-10}\ \mu_B$ when reactor data were added. The results indicate the role of reactor experiments in constraining the magnetic moment effects.

5. FUTURE PROJECTS AND PROSPECTS

The sensitivities for neutrino magnetic moments in direct search experiments scale as

$$\mu_\nu \propto \frac{1}{\sqrt{N_\nu}}\ [\frac{B}{M\ t}]^{\frac{1}{4}} \qquad (5)$$

where N_ν is the signal events at some reference magnetic moments, B, M, t are the background level, detector mass and measurement time, respectively. The best strategy to enhance the sensitivities is to increase on N_ν, which is proportional to the neutrino flux ϕ_ν and is related to the detection threshold in recoil energy T.

The atomic energy level effects[22] limit the potential sensitivity improvement by reducing T only. For example, N_ν only increases by a factor of three with a lowering of detection threshold from 10 keV to 10 eV in germanium. Therefore, big statistical boost in μ_ν will most favorably be achieved by an increase in ϕ_ν – while keeping the systematics in control via (a) lowering the detection threshold to retain the "$\mu_\nu \gg SM$" event-rate requirements, and (b) maintaining a low background level. Since the minimal energy transfer to the atomic electrons would be ∼100 eV, it follows from condition (a) that such an approach of enhancing ϕ_ν and reducing T may only be applicable for $\mu_\nu \to 10^{-13}\ \mu_B$.

The GEMMA experiment[23] under preparation at the Kalininskaya Nuclear Reactor in Russia is similar to the TEXONO-KS approach, aiming at an improvement to $\mu_\nu(\bar{\nu_e}) \to 3\times10^{-11}\ \mu_B$ by locating at a closer distance, using a larger mass target and operating at a lower threshold. The MAMMONT project[24], currently at the R&D phase, has ambitious specifications of deploying a 40 MCi(4 kg) tritium source with a flux of $6\times10^{14}\ cm^{-2}s^{-1}$ on ultra-sensitive detectors with threshold down to 10 eV, either with cryogenic silicon detectors or germanium with internal amplification. The projected sensitivity is $\mu_\nu(\bar{\nu_e}) \to 2.5\times10^{-12}\ \mu_B$.

The TEXONO Collaboration continued data taking with the HPGe at KS. Sensitivities to the $\sim 10^{-10}\ \mu_B$ range can be expected. In parallel, a CsI(Tl) crystal scintillator array[25] with a total

mass of 200 kg is collecting data. The focus is on the high(>3 MeV) recoil energy range to perform a first measurement of SM neutrino-electron scattering at the MeV momentum transfer range. A 5 g "ultra-low-energy" germanium prototype is being tested, where the goal is to develop into an 1 kg Ge-array detector for the first experimental observation of neutrino-nucleus coherent scattering. As by-product, such an experiment will potentially probe $\mu_\nu(\bar{\nu_e}) \to 2\times10^{-11}\ \mu_{\rm B}$. An energy threshold of 100 eV has been demonstrated[26] with the prototype while background studies at the sub-keV range are under way.

Alternatives of neutrino sources such as artificial radioactive sources[27], and accelerator-based β-sources have been discussed, projecting a sensitivity range of $\sim$few$\times10^{-11}\ \mu_{\rm B}$ in both cases.

6. OUTLOOK

The magnetic moments of the neutrino parametrize how it couples to the photons and are sensitive to its masses and mixings, as well as its Dirac or Majorana nature. It is, therefore, a *conceptually* rich subject with much neutrino physics and astrophysics to be explored. However, there are no indications of any measurable/observable signals in the current and future rounds of experimental efforts. Improvement in sensitivities will necessarily involve new neutrino sources as well as novel neutrino detection techniques and channels. These advances may find important potential applications in other areas of neutrino and underground physics experimentations.

REFERENCES

1. See the respective sections in Review of Particle Physics, Particle Data Group, Phys. Lett. **B 592** (2004), for details and references.
2. See these proceedings for updates.
3. A. de Gouvea, these proceedings.
4. B. Kayser, Phys. Rev. **D 26**, 1662 (1982); J.F. Nieves, Phys. Rev. **D 26**, 3152 (1982).
5. P. Vogel and J. Engel, Phys. Rev. **D 39**, 3378 (1989), and references therein.
6. R.N. Mohapatra, S.P. Ng, H.B. Yu, hep-ph/0404274 (2004).
7. G.G. Raffelt, "Stars as Laboratories for Fundamental Physics", Sect. 7.5, U. Chicago Press (1996).
8. G.G. Raffelt, Phys. Rev. **D 39**, 2066 (1989).
9. J. Barranco et al., Phys. Rev. **D 66**, 093009 (2002), and references therein.
10. K. Eguchi et al., Phys. Rev. Lett. **92**, 071301 (2004).
11. E.Kh. Akhmedov and J. Pulido, Phys. Lett. **553**, 7 (2003); O.G. Miranda et al., Phys. Rev. Lett. **93**, 051304 (2004).
12. D.W. Liu et al., Phys. Rev. Lett. **93** 021802, (2004).
13. H.O. Back et al., Phys. Lett. **B 563**, 35 (2003).
14. J.A. Grifols, E. Masso and S. Mohanty, Phys. Lett. **B 587** 184 (2004).
15. L.B. Auerbach et al., Phys. Rev. **D 63**, 112001 (2001).
16. R. Schwienhorst et al., Phys. Lett. **B 513**, 23 (2001).
17. F. Reines, H.S. Gurr and H.W. Sobel, Phys. Rev. Lett. **37**, 315 (1976).
18. Z. Daraktchieva et al., Phys. Lett. **B 564**, 190 (2003).
19. H.B. Li and H.T. Wong, J. Phys. **G 28**, 1453 (2002).
20. H.B. Li et al., Phys. Rev. Lett. **90**, 131802 (2003), and references therein.
21. W. Grimus et al., Nucl. Phys. **B 648**, 376 (2003); M.A. Tortola, hep-ph/0401135 (2004).
22. V.I. Kopeikin et al., Phys. Atom. Nucl. **60**, 2032 (1997).
23. A.G. Beda et al., Phys. Atom. Nucl. **61**, 66 (1998).
24. L.N. Bogdanova, Nucl. Phys. **A 721** 499 (2003)
25. H.T. Wong et al., Astropart. Phys. **14**, 141 (2000); Y. Liu et al., Nucl. Instrum. Methods **A 482**, 125 (2002).
26. H.T. Wong, Mod. Phys. Lett. **A 19**, 1207 (2004).
27. I.R. Barabanov et al., Astropart. Phys. **8**, 67 (1997); A. Ianni and D. Montanino, Astropart. Phys. **10**, 331 (1999).
28. G.C. McLaughlin and C. Volpe, Phys. Lett. **B 591**, 229 (2004); C. Volpe, these proceedings.